Surface Interactions with Adsorbed Macromolecules[1]

JACOB KLEIN

Polymer Research Department, Weizmann Institute of Science, Rehovot, Israel

Received October 9, 1985; accepted October 29, 1985

Surface interactions, as revealed by surface force studies between mica sheets in 0.1–0.2 M KNO_3 aqueous electrolyte, are critically examined for three different types of macromolecules adsorbed on the surfaces: flexible uncharged polymer, flexible charged polyelectrolyte, and rigid rod protein. Aspects of specific and nonspecific effects, such as surface conformation, the origin of repulsive interactions and the possibility of attractive bridging, as well as the question of equilibrium and reversibility for such adsorbed macromolecular layers, are compared and contrasted.

I. INTRODUCTION

The forces acting between two solid surfaces across a liquid medium may be profoundly modified by the adsorption of macromolecules on the surfaces, even at adsorbances of well below a "macromolecular monolayer" (1, 2). The essential reason for this is that the range of field-type forces acting between "bare" surfaces (such as attractive dispersion forces, or repulsive long-ranged electrostatic double-layer effects) is comparable with, or less than, the thickness of the adsorbed macromolecular layers; the interactions then become characteristic of those between the adsorbed phase rather than the adsorbing substrate. Figure 1 illustrates this schematically, for both flexible polymers and rigid macromolecules, such as proteins.

Over the past few years we have studied interactions between atomically smooth mica surfaces immersed in liquids, both in the absence and in the presence of macromolecules adsorbed onto the surfaces from the solution. In this way the modification of the surface forces induced by the adsorbed layers was determined directly in a variety of different conditions. These include the use of flexible uncharged polymers of different molecular weights in different solvency conditions, charged polymers, surfactants, and rigid rod-like proteins, and also the use of both aqueous and nonaqueous solvents as media (3–8). In addition we were able to control the extent of adsorbance of macromolecules during an experiment, and so to characterize the effect of surface coverage on the surface–surface interactions (7, 9).

The experimental technique used is based on multiple-beam interferometry to measure the separation between the mica sheets, and was pioneered by Tabor and co-workers in Cambridge for surface forces in air and under vacuum (10, 11), and later extended by Isrelachvili and co-workers in Australia for surfaces immersed in liquid media (12). The geometry is that of crossed-cylinders, of radii R_1 and R_2 (R_1, $R_2 \simeq 1$ cm), a closest distance D apart (Fig. 2). By measuring the separation D between them (in the convenient range 0–3000 Å, with a resolution of ±3 Å) while independently moving one of the surfaces by known amounts, the force $F(D)$ between them is directly determined from the bending of a leaf spring supporting the other surface (3, 12). In order to compare results of different experiments, the Derjaguin approximation (13) is used, where

[1] Presented at the 5th International Conference on Surface and Colloid Science, Clarkson University, Potsdam, N.Y., June 24–26, 1985, as part of a symposium entitled Protein and Polyelectrolyte Adsorption.

0021-9797/86 $3.00

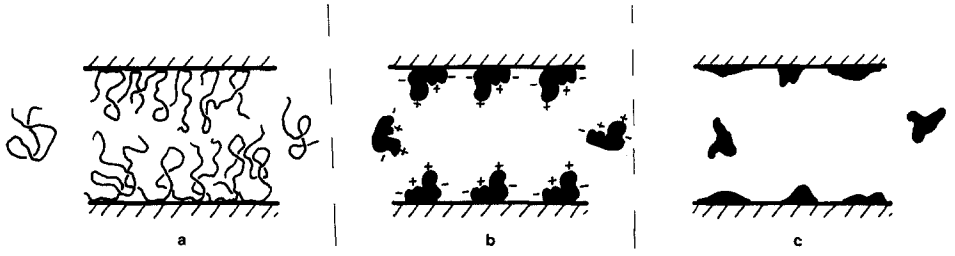

FIG. 1. Schematic illustration of macromolecular adsorption. (a) Nonspecific adsorption of flexible, uncharged polymers. (b) Adsorption of rigid macromolecules in specific surface orientations. (c) Adsorption of rigid macromolecules with consequent deformation.

$$F/2\pi\sqrt{R_1R_2} = E(D) \qquad [1]$$

gives the surface energy per unit area $E(D)$ between two flat parallel plates a distance D apart, obeying the same force–distance law $F(D)$. In this way the effect of different curvatures R_1, R_2 (in different experiments) is normalized out, and contact can be made with theoretical models in which it is $E(D)$ that is usually evaluated (2). In addition, the optical technique allows a simultaneous measure of the mean refractive index $n(D)$ of the medium in the gap between the surfaces: this gives a measure of the adsorbance on the surfaces (3).

In this paper we examine specific and nonspecific features of forces between surfaces, as revealed by the force–distance profiles, which are the primary output of our investigations.

II. SPECIFIC AND NONSPECIFIC SURFACE FORCES

Field-type interactions between smooth solid surfaces across a liquid include attractive van der Waals forces, and possible repulsive forces due to formation of electrostatic double-layers (in ionic media) arising from ion adsorption onto the surfaces; these constitute the basic ingredients of the generally successful DLVO theory of colloidal stability (14, 15). In addition, at surface separations up to several diameters of the liquid molecules, the affinity of liquid to the surface (16) (solvation effects) and possible ordering of molecular layers close to the interface (17) may lead to a repulsive contribution (though in the present discussion we shall be considering surface separations where such effects are unimportant). The adsorption of macromolecules at the solid–liquid interface brings into play a different set of factors (1).

It is convenient to divide these into specific and nonspecific effects: the former are more likely to be found in the case of adsorbed rigid or charged macromolecules (such as proteins, which have a very specific structure) in polar media (18). They include electrostatic interactions between opposing adsorbed species which may be sensitive to the relative configuration of the (rigid) macromolecules with respect to the surface and to each other (for example, specific functional groups may be preferentially adsorbed, or repelled, by a given surface: their contribution to the surface–surface forces will then be suppressed, or enhanced), as sketched in (Fig. 1b); possible distortion by the surface of a rigid macromolecular structure, with consequent rearrangement of interacting sites and polymer dimensions, as sketched in Fig. 1c; and surface–surface in-

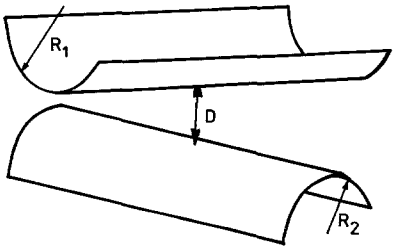

FIGURE 2

teraction characteristics which are strongly history-dependent (for example, if the adsorbed layers have been previously compressed). Clearly, in order to interpret the results of model studies on surface interactions which involve such specific effects, it is important to have detailed information on the configuration of the surface-adsorbed macromolecules.

Nonspecific effects with adsorbed macromolecules are those usually associated with uncharged polymers (Fig. 1a), with identical monomers strung along an essentially linear flexible backbone. They include osmotic interactions between opposing adsorbed segments (whose sign and magnitude depend on solvent "goodness"); repulsive effects associated with entropy reduction arising from volume exclusion due to the impermeable adsorbing substrates at small surface separations; and attractive "bridging" which occurs when a given polymer is adsorbed simultaneously on both surfaces spanning the gap between them (9). Comprehensive reviews have been given (1, 2). The adsorbed polymers adopt a wide range of configurations which are continually interchanging, and both the interpretation of model investigations and theoretical calculations can rely on a statistical approach, which does not need detailed knowledge of specific configuration. This is because even when the detailed surface–monomer interactions differ from one case to the other, and highly specific configurations may be obtained very close to the solid–liquid interface itself, the effect of this on the overall polymer configuration decays beyond a few statistical steps of the flexible chain away from the adsorption site. In addition, surface interactions in such systems generally exhibit a quasiequilibrium behavior which is not history dependent, once adsorption has taken place; the adsorption process itself, however, is often effectively irreversible due to the large binding energies involved per molecule. In the following sections we contrast specific and nonspecific features, in surface interaction phenomena, in systems with adsorbed charged and rigid molecules with those bearing flexible, uncharged polymers.

III. REVERSIBILITY, RANGE, AND RELAXATION EFFECTS

Figures 3–5 show force–distance profiles between mica sheets bearing three different types of macromolecules: (a) an uncharged, flexible polymer, polyethylene oxide (PEO) (taken from Ref. (4)); (b) a polyelectrolyte, poly-L-lysine, which is fully ionized in the aqueous electrolyte medium (taken from Ref. (6)); (c) a rigid biological macromolecule, monomeric (calf-skin) collagen (19) (taken from Ref. (3)). Their molecular characteristic are given in the figure legends. In all cases the medium is aqueous KNO_3, of molarity 0.1, 0.1, and 0.2 M for (a), (b), and (c), respectively. We focus here on the three features noted in the section heading, and the contrast between the three systems.

(a) Polyethylene Oxide

The solid line A in Fig. 3 represents the quasiequilibrium or "relaxed" force law for this system: following overnight incubation of the mica surfaces in the PEO solution they are brought together and the force profile A is followed up to the point of closest approach C. If they are slowly taken apart (or decompressed; around 1 h for the surface separation D to go from 6 to 200 nm) curve A is again followed; subsequent compression again follows curve A. However, if the surfaces are compressed to C and then rapidly withdrawn (some 5 min for D going from 6 to 200 nm, this being the time necessary for measurements) then force profile B (broken curve) is indicated; and immediate subsequent recompression again follows curve B. On the other hand, if a rapid decompression is followed by a "waiting time" of $\frac{1}{2}$ h or longer, then once again profile A is followed on compression. Intermediate rates of compression and decompression fall between the "relaxed" curve A and the "unrelaxed" curve B. The central point however is the existence of

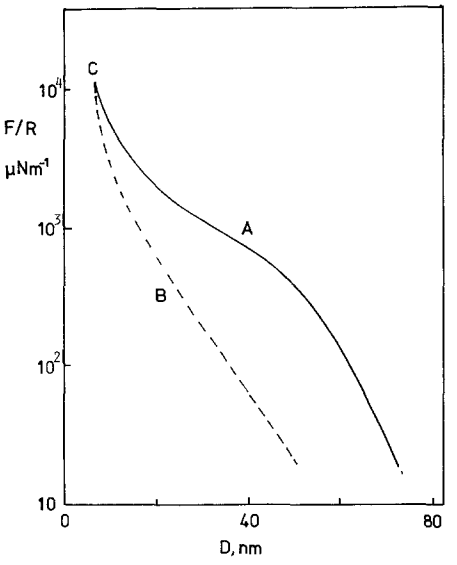

FIG. 3. Interaction–distance profile between mica surfaces (geometry as Fig. 2, $R = \sqrt{R_1 R_2}$) following overnight incubation in a dilute solution of monodispersed polyethylene oxide $(-CH_2-CH_2-O-)_n$, of molecular weight $M = 1.6 \times 10^5$, in aqueous 0.1 M KNO_3. Solid curve A and broken curve B represent the "relaxed" and "unrelaxed" limits (see also text). Taken from Ref. (4).

a quasiequilibrium force law at sufficiently low rates of surface compression, corresponding to curve A.

(b) Poly-L-lysine

An entirely different behavior is exhibited by the charged poly-L-lysine layers, shown in Fig. 4a. The broken curve A represents the force profile on a first approach following overnight incubation, to the point of closest approach C. On decompression, however, at whatever rate,the force profile follows dotted curve B, very much closer in: subsequent compression and decompression force profiles all fall (within error) on curve B. Thus an irreversible distortion of the adsorbed poly-L-lysine appears to take place following the first compression: no relaxation of the surface layers occurs following this first approach of the surfaces, even when they are subsequently held far apart in solution for many hours. This is in sharp contrast to the case of the adsorbed PEO (Fig. 3), where for time scales of over ca. 1 h the behavior always reverts to its "relaxed" value (curve A, Fig. 3). The experimental approach moreover allows us to determine that it is not desorption of the polyelectrolyte which is responsible for the "moving in" of the force profile following a first compression: Fig. 4b shows the refractive index profile $n(D)$ deter-

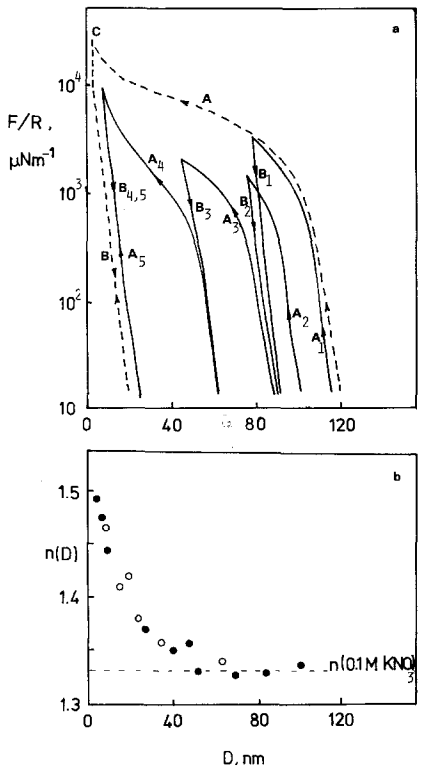

FIG. 4. (a) Interaction–distance profile between mica surfaces following overnight incubation in a dilute solution of poly-L-lysine,

$$(-CH-CH-CO-)_n,$$
$$\quad\quad|$$
$$\quad(CH_2)_4NH_4^{\oplus}$$

$M = 9 \times 10^4$ ($n \simeq 700$), in aqueous 0.1 M KNO_3. The broken curve is the single-stage compression (A) and decompression (B) profile. The solid curves are for a multistage compression–decompression profile. Broken curve B also represents the final behavior of the system following compression (see text). (b) Refractive index profile for the adsorbed polylysine. (●) First compression (corresponding to curve A on force profile, (a)). (○) Second compression (corresponding to curve B on force profile, (a)). Taken from Ref. (6).

mined during both first and subsequent compressions, and shows that, within error, $n(D)$ remains unchanged. This implies that the amount of polymer within the gap remains constant.

The solid curves A_n, B_n in Fig. 4 show the behavior during a multistage compression–decompression cycle for the mica sheets with adsorbed polylysine; curve A_1 is a first *partial* compression following initial incubation, and B_1 is the corresponding *decompression* curve; the surfaces are then taken a long way apart and brought in again, whereupon initial repulsion begins closer in, and follows curve A_2; B_2 is the corresponding decompression force profile, and so on down to the position of the single-step decompression profile (broken line), following which all subsequent compression/decompression curves lie on that profile. This experiment clearly shows the progressive nature of the irreversible compression of the adsorbed polylysine layers. It has been interpreted in terms of an initial configuration of the adsorbed polyelectrolyte which is metastable and highly extended from each surface due to a space-charge region within the adsorbed layer. On mechanical compression more (positively charged) lysine monomers are forced onto the (negatively charged) mica surfaces, there to adhere strongly and quasiirreversibly. Clearly, such an interpretation requires additional information—for example, on the coverage of the substrate by surface-bound monomers—for confirmation. Such information must come from independent surface analysis studies.

(c) Monomeric Collagen

Figure 5 shows the results of preliminary force-measurements between mica sheets following incubation (for two concentrations) in monomeric collagen solution, taken from Ref. (3). A rapid initial rise in repulsive force commencing at $D \simeq 650$–700 nm is followed by a flatter rise (on a log–linear plot) down to 20–30 nm. Decompression from the point of closest approach results in rapid fall-off of the repulsion, and subsequent approaches indicate an onset of repulsion occurring considerably further in then 700 nm. Though we did not investigate this behavior in as much detail as in the model polypeptide (poly-L-lysine) study, both the shape of the force profile and the irreversible nature of the compressive distortion are similar for these charged macromolecules (one flexible, the other a rigid rod), and differ qualitatively from the case of the uncharged PEO.

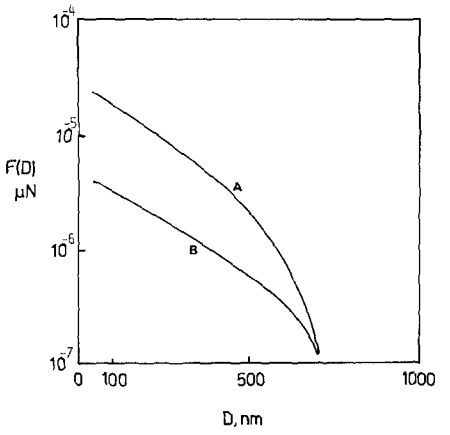

FIG. 5. Force profile between mica sheets following overnight incubation in dilute solution of monomeric collagen in aqueous 0.2 M KNO_3, for two different solution concentrations. Curve A, 10 $\mu g \cdot ml^{-1}$; curve B, 1.8 $\mu g \cdot ml^{-1}$. Taken from Ref. (3).

Two further features in the force profiles for the above systems deserve comment: the range of interactions between the macromolecule-bearing substrates and the origin of the repulsions. If we take the separation D at onset of repulsion as a measure of twice each adsorbed layer thickness δ, we find that for PEO this thickness $D = 2\delta \simeq 80$ nm corresponds to $\delta \simeq 3R_g$, where R_g is the unperturbed radius of gyration of the PEO sample of Fig. 3 ($M = 1.6 \times 10^5$, $R_g = 13$ nm). Adsorbed PEO samples of different M values, in the range 4×10^4–1.2×10^6 also exhibit similar layer thicknesses (i.e., 3–4 R_g for the respective polymers) characteristic of flexible polymers adsorbed in good solvent systems (1). (0.1 M KNO_3 is a moderately good solvent for the PEO.) For the

poly-L-lysine onset of interaction is at around $D = 120$ nm, corresponding to $\delta \simeq 7$–$8R_g$ for this sample ($M = 90{,}000$, $R_g \simeq 8$ nm) or over twice that for the uncharged polymer in terms of unperturbed dimensions. This is in line with what one expects of fully ionized polyelectrolytes in solution, where mutual charge repulsion leads to chain extension; we note however that the *fully extended* polypeptide chains would be some $37R_g$ in length for this sample, so that a considerable degree of coiling is indicated for the adsorbed polyelectrolyte. Finally, we note the range for onset of repulsion in the case of the rigid collagen monomers is $D \simeq 650$ nm or some twice the rod length of this protein (19) (length $\sim$ 300 nm, diameter $\sim$ 2 nm); this suggests that the proteins are adsorbed standing end-on on the mica substrate. This observation is corroborated by viscometric studies of the hydrodynamic thickness (ca. 400 nm) of glass-adsorbed collagen monomer (20); and especially by radiometric measurements (21) on adsorption of radiolabeled monomeric collagen onto glass and mica: these showed an adsorbance of ~ 1 mg $\cdot$ m^{-2}, which rules out any thick, multilayer, side-on adsorption of the collagen, and suggests a rather sparse "forest" of collagen rods sticking out from the surface. This is considerably different from both the PEO and polylysine adsorption modes, and suggests a behavior highly specific to this rod-like protein.

The origin of the repulsive forces for the two ionized adsorbed species (Figs. 4, 5) is indicated by the F vs D variation in the *initial* stages of the interaction: in this regime the force varies as

$$F \propto e^{-\kappa D}$$

for both the collagen and the flexible polypeptide: the value of $1/\kappa$ ($\simeq$1 nm) corresponds closely to the Debye screening length (14, 15) expected for electrostatic (double-layer) repulsion at the ionic strengths (0.1–0.2 M KNO_3) of the aqueous electrolyte. Thus these initial stages are dominated by the electrostatic interactions between the macromolecule-bearing mica surface. For PEO, on the other hand, the initial rise in $F(D)$, which is also quasiexponential, has a "decay-length" of some 8 nm, very different to the Debye screening length at 0.1 M KNO_3. The repulsion for the PEO then is of different origin; it is associated with osmotic repulsion between opposing segments in the good solvent medium.

IV. LONG-RANGE ATTRACTIVE SURFACE FORCES

One unique mode by which adsorbed flexible polymers may modify surface interactions is that of bridging: when a single polymer is simultaneously adsorbed on both surfaces, spanning the gap between them, as indicated schematically in Fig. 6. The contribution of such bridging is always attractive (1); in good solvent conditions there is in addition a repulsive component resulting from the osmotic interactions of polymer segments within the gap, and the net force acting between the surfaces depends on the relative magnitudes of the bridging and the osmotic effects. Broadly speaking, for polymer volume fractions ϕ in the intersurface gap, the contribution of (attractive) bridging goes approximately as ϕ, while that of the osmotic repulsion goes approximately as ϕ^2 (for a given separation D, and making the zero-order assumption that ϕ is uniform across the gap). Thus at sufficiently low ϕ (and hence low adsorbance) bridging attraction should be the dominant effect, even in good solvent conditions.

Recently, together with Paul Luckham, we measured surface forces between mica sheets immersed in a solution of high-molecular-weight PEO ($M = 1.2 \times 10^6$) in 0.1 M KNO_3 aqueous electrolyte under conditions where

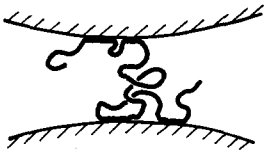

FIG. 6. Schematic illustration of "bridging."

the amount of polymer adsorbed could be limited to low values. This was done by maintaining the surfaces very close together ($D \sim 20$ μm) during the incubation in solution so that the rate of polymer adsorbance was severely diffusion limited. The results of such a study, at progressively longer incubation times—corresponding to increasing amounts of polymer adsorbed and in the gap—are shown in Fig. 7, based on Ref. (9). Figure 7, curve (a), shows the force profile in the absence of polymer, indicating little interaction down to ca. 15 nm where a weak attraction is observed, due to van der Waals forces between the bare mica substrates. Following addition of polymer (to a few ppm) and 1 h incubation, the short-range attraction disappears (Fig. 7b), to be replaced, after a further 2 h in the solution, by a marked, long-ranged ($\gtrsim$100 nm, or some $3R_g$ for this polymer) attraction Fig. 7c). This attraction persists for up to about 6 h incubation (longer incubation corresponding to more adsorbed polymer on the surface); at longer time, it disappears to be replaced by a monotonic repulsion which becomes progressively longer ranged (Fig. 7, curves d and e) up to a limit (after about 24 h incubation) of $D \simeq 6R_g$ ($=2\delta$), similar to the case of the fully adsorbed PEO in Fig. 3.

These results represent the first direct observation of long-ranged attraction between substrates bearing an adsorbed flexible polymer in *good solvent* conditions, i.e., where the osmotic interaction between the segments is repulsive. They strongly indicate a "bridging" phenomenon, as in Fig. 6; they also have implications for our understanding and control of flucculation/stabilization processes in colloidal dispersions with adsorbed polymers. For example, the minimum in the attractive well (at $D = D_{min}$) in Fig. 7c, when translated to the case of two colloidal particles (size 1 μm) obeying the same force law $F/R = 2\pi E(D)$, corresponds to a total adhesive energy between them of some 20 kT when they are a distance D_{min} apart. Such particles, once adhered, would not readily be forced apart again by thermal fluctuations (of energies $\sim$ 1 kT). Since, as also shown by our experiments, little additional polymer makes its way into the gap once the surfaces are close together ($D \simeq D_{min}$), the adhered particles would effectively be permanently aggregated.

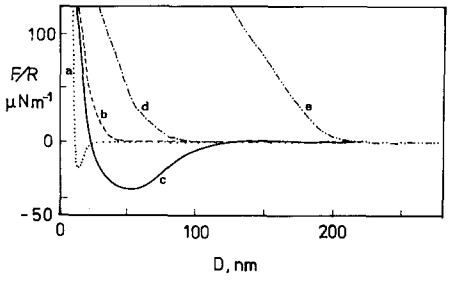

FIG. 7. Interaction between mica surfaces in 0.1 M aqueous KNO_3 solution (curve a), and after progressively longer incubation times at $D \simeq 20$ μm, following addition of polyethylene oxide ($M = 1.2 \times 10^6$) to the solution. Incubation: curve b, 1 h; curve c, 3 h; curve d, 8 h; curve e, 32–48 h. Taken from Ref. (9).

Does such bridging play a role in the case of adsorbed polyelectrolytes? This question is of particular interest in the context of cellular and biocolloidal systems, as well as in synthetic dispersions in ionic media. Living cells frequently synthesize and secrete flexible polyelectrolytes, such as polysaccharides (22) for example, hyaluronic acid), and in addition have a variety of macromolecular species incorporated into the cell membrane surface (18, 23). Thus bridging effects may be of relevance to (nonspecific), long range cell–cell adhesion and membrane–membrane interaction processes. Very recently, Chris Toprakcioglu, together with Paul Luckham and myself, has examined the variation of surface forces between mica sheets immersed in a solution of poly-L-lysine in aqueous electrolyte, where—as for the case of PEO, Fig. 7—the rate of polypeptide adsorption was severely diffusion-limited. The situation here is inherently more complicated than with the uncharged PEO, as one might expect the adsorbance of the ionized poly-L-lysine to change the mica surface potential as it adsorbs. Nonetheless preliminary data do suggest that, over a limited adsorbance regime, long-range bridging attraction due to

polyelectrolyte molecules spanning the mica–mica gap may be the dominant mode. Further experiments on this system are in progress.

V. SUMMARY AND CONCLUDING REMARKS

The measurement of forces between two atomically smooth surfaces across a liquid medium provides a singularly direct experimental means for studying the modification of surface interactions by adsorbed macromolecules. The useful range of the technique, up to a few hundred nanometers, is about an order of magnitude larger than the extension from each surface of typical adsorbed macromolecular layers; in addition, the regime of surface separation of interest for interactions with adsorbed macromolecules is generally greater than about 5 nm: this allows interpretation of the force profiles uncomplicated by very-short-range structural and solvation effects near the smooth substrates. The information on the *adsorbance,* available simultaneously from refractive index data, provides an additional dimension to the investigations.

Comparison of force profiles for uncharged and charged flexible polymers and a rigid rod-like protein shows different characteristics for the three cases. In particular, the adsorbed layers in the case of the charged macromolecules, though very extended following initial adsorption, appear to undergo an irreversible compression after a first approach, while the flexible uncharged polymer behaves reversibly over sufficiently long time scales. A nonspecific feature which appears common to both the charged and uncharged flexible polymers is that of long-ranged, net bridging attraction—though this is manifested only over a narrow range of adsorbance. These and other contrasting features are summarized for the three systems in Table I.

Finally, it is important to bear in mind that in this technique one is essentially integrating effects measured over surface areas very much larger than either the range of the interactions or the size of the adsorbed molecules (the radii of the curved mica sheets are around 1 cm). While this makes the technique very suitable for measuring, and interpreting, nonspecific effects, especially for flexible uncharged polymers, care must be taken in the case of rigid (or even flexible) charged macromolecules. In these systems the specific configuration at the solid–liquid interface may have a profound effect on the overall measured interactions (unlike for flexible uncharged polymers where these effects decay rapidly away from the interface): interpretation of force profiles in this case requires detailed knowledge of the configuration of the adsorbed species. It is probably most directly obtained using other surface-sensitive techniques (24).

TABLE I

Summary of Adsorption and Surface Interaction Features (Mica Surfaces in 0.1 *M* KNO_3)

Macromolecule	Quasi-irreversibly adsorbed	Initial interaction	Net bridging attraction at low adsorbance	Extension δ of adsorbed layer	Relaxation of surface layers following compression
Uncharged, flexible (polyethylene oxide)	✓	Repulsive osmotic	✓	$\delta \simeq 3 \pm 1 R_g$	Yes
Charged, flexible (poly-L-lysine)	✓	Repulsive-electrostatic double layer	?	$\delta \simeq 8 R_g$ initially	No
Charged, rigid (collagen rods)	✓	Repulsive	?	End-on adsorption initially $\delta \simeq$ 300–350 nm	No

ACKNOWLEDGMENTS

The collaboration of Dr. P. F. Luckham and Dr. C. Toprakcioglu in the surface–force studies described in this paper is gratefully acknowledged.

REFERENCES

1. Vincent, B., *Adv. Colloid Interface Sci.* **4,** 193 (1974).
2. Vincent, B., and Whittington, S. G., *Surf. Colloid Sci.* **12,** 1 (1982).
3. Klein, J., *Nature (London)* **288,** 248 (1980); *J. Chem. Soc. Faraday 1* **79,** 99 (1983).
4. Klein, J., and Luckham, P. F., *Nature (London)* **300,** 429 (1982); *Macromolecules* **17,** 1041 (1984).
5. Israelachvili, J. N., Tirrell, M., Klein, J., and Almog, Y., *Macromolecules* **17,** 204 (1984).
6. Luckham, P. F., and Klein, J., *J. Chem. Soc. Faraday 1* **80,** 865 (1984).
7. Almog, Y., and Klein, J., *J. Colloid Interface Sci.* **106,** 33 (1985).
8. Luckham, P. F., and Klein, J., *Macromolecules* **18,** 721 (1985).
9. Klein, J., and Luckham, P. F., *Nature (London)* **308,** 836 (1984).
10. Tabor, D., and Winterton, R. H. S., *Proc. R. Soc. London Ser. A* **312,** 435 (1968).
11. Israelachvili, J. N., and Tabor, D., *Proc. R. Soc. London Ser. A* **331,** 19 (1971).
12. Israelachvili, J. N., and Adams, G., *J. Chem. Soc. Faraday 1* **74,** 975 (1978).
13. Derjaguin, B. V., *Kolloid Zh.* **69,** 155 (1934).
14. Derjaguin, B. V., and Landau, J., *Acta Physicochim. URSS* **14,** 633 (1941).
15. Vervey, E. J. W., and Overbeek, J. G., "Theory of the Stability of Lyophobic Colloids." Elsevier, Amsterdam, 1948.
16. Le Neveu, D., Rand, R. P., and Parsegian, V. A., *Nature (London)* **259,** 601 (1976).
17. Horn, R. G., and Israelachvili, J. N., *J. Chem. Phys.* **75,** 1400 (1981).
18. Hair, M., Ed., "The Chemistry of Biosurfaces." Decker, New York, 1971.
19. Traub, W., and Piez, K. A., *Adv. Protein Chem.* **25,** 243 (1971).
20. Silberberg, A., and Klein, J., *Biorheology* **18,** 589 (1981).
21. Penners, G., Priel, Z., and Silberberg, A., *J. Colloid Interface Sci.* **80,** 437 (1981); Penners, G., unpublished data.
22. Comper, W. D., and Laurent, T. C., *Physiol. Rev.* **58,** 255 (1978).
23. Bell, G. J., *Science* **200,** 601 (1978).
24. Iwamoto, G. W., Van Wagenen, R. A., and Andrade, J. D., *J. Colloid Interface Sci.* **86,** 581 (1982).